nature biotechnology

LETTERS

https://doi.org/10.1038/s41587-019-0373-y

Generation of human endothelium in pig embryos deficient in *ETV2*

Satyabrata Das[1,6], Naoko Koyano-Nakagawa[1,2,6], Ohad Gafni[1], Geunho Maeng[1], Bhairab N. Singh[1], Tara Rasmussen[1], Xiaoyan Pan[1], Kyung-Dal Choi[1], Daniel Mickelson[1], Wuming Gong[1], Pruthvi Pota[1], Cyprian V. Weaver[1], Stefan Kren[1], Jacob H. Hanna[3], Demetris Yannopoulos[1,4], Mary G. Garry[1,4,5,7*] and Daniel J. Garry[1,2,4,5,7*]

The scarcity of donor organs may be addressed in the future by using pigs to grow humanized organs with lower potential for immunological rejection after transplantation in humans. Previous studies have demonstrated that interspecies complementation of rodent blastocysts lacking a developmental regulatory gene can generate xenogeneic pancreas and kidney[1,2]. However, such organs contain host endothelium, a source of immune rejection. We used gene editing and somatic cell nuclear transfer to engineer porcine embryos deficient in *ETV2*, a master regulator of hematoendothelial lineages[3–7]. *ETV2*-null pig embryos lacked hematoendothelial lineages and were embryonic lethal. Blastocyst complementation with wild-type porcine blastomeres generated viable chimeric embryos whose hematoendothelial cells were entirely donor-derived. *ETV2*-null blastocysts were injected with human induced pluripotent stem cells (hiPSCs) or hiPSCs overexpressing the antiapoptotic factor BCL2, transferred to synchronized gilts and analyzed between embryonic day 17 and embryonic day 18. In these embryos, all endothelial cells were of human origin.

Previous studies have described the generation of xenogeneic organs in rodents by injection of pluripotent stem cells (PSCs) into blastocysts lacking a developmental regulatory gene for the organ of interest. Injection of wild-type rat PSCs into mouse blastocysts lacking *Pdx1* resulted in the generation of a fully functional rat pancreas in *Pdx1*-null mice[1]. Similarly, it has been reported that human PSCs can engraft and differentiate to multiple lineages in pig embryos after blastocyst complementation[8]. However, the resulting chimeric organs still retain a host-derived endothelium capable of eliciting a hyperacute (immediate) rejection following the exposure of the recipient's blood to the transplanted chimeric organ[1,2]. Here we sought to engineer animals that have an exogenous endothelial lineage to circumvent acute organ rejection. Our laboratory and others have established that ETV2 is a master regulator of hematoendothelial lineages[3–7]. ETV2 belongs to the Ets family of transcription factors and plays a non-redundant role in the specification of haematopoiesis and vasculogenesis. *Etv2*-deficient mouse embryos die early during embryogenesis and completely lack hematoendothelial lineages[3–5,9]. We undertook studies in mice and pigs to determine whether embryo complementation with PSCs could, in a cell-autonomous fashion, rescue *ETV2*-mutant embryos through the generation of donor-cell-derived hematoendothelial cells.

First, we used mouse embryonic stem (ES) cells and embryoid body formation to evaluate the mesodermal potential of ES cells[4–7]. We differentiated the enhanced yellow fluorescent protein (EYFP)-labeled wild-type mouse ES cell line 7AC5 (ref. [10]) and unlabeled wild-type and *Etv2*-null mouse ES cells either separately or in combination, and evaluated the induction of endothelial ($FLK1^+TIE2^+$) and hematopoietic ($CD41^+$) lineage markers using flow cytometry (Supplementary Fig. 1a,b). Differentiation of EYFP-labeled wild-type cells alone resulted in expression of EYFP by more than 95% and 94% of the endothelial and hematopoietic cells, respectively (approximately 5% of the differentiated cells did not express EYFP suggesting that some cells silenced EYFP expression). Similarly, when EYFP-labeled wild-type cells were co-cultured with *Etv2*-null cells, 94% and 92% of the endothelial and hematopoietic populations, respectively, expressed EYFP, and the lineage differentiation was indistinguishable from that of EYFP-labeled wild-type cells alone (Supplementary Fig. 1a–c). We then undertook embryo complementation studies by using the *Etv2*-null mouse model. Hemizygous mice for two different *Etv2*-mutant lineages $Etv2^{KO/+}$ (ref. [4]) and $Etv2^{dKI/+}$ (ref. [11]) were bred to generate compound $Etv2^{dKI/KO}$ knockout embryos. As this compound mutant can be identified genotypically by the presence of each mutant allele, null embryos can be unambiguously identified by the presence of wild-type complementing cells. We isolated blastocysts from these compound mutants, complemented them with EYFP-labeled wild-type ES cells and implanted them in pseudopregnant dams. Immunohistochemical and fluorescence-assisted cell sorting (FACS) analyses revealed that the complemented chimeric *Etv2*-null mouse embryos were viable and that the endothelial and hematopoietic lineages were rescued. Furthermore, we demonstrated in these chimeric embryos that the hematoendothelial lineages were entirely $EYFP^+$ (Supplementary Figs. 1d–s and 2a–d), supporting the notion that complementation is cell autonomous and that wild-type mouse ES cells can rescue the *Etv2*-null mouse phenotype.

To generate porcine embryos for endothelial and hematopoietic replacement (Supplementary Fig. 3), we examined whether the porcine *ETV2*-null embryo phenocopied the mouse mutants and lacked hematoendothelial lineages. We deleted the *ETV2* gene in a biallelic fashion in porcine embryonic fibroblasts by using

[1]Department of Medicine, University of Minnesota, Minneapolis, MN, USA. [2]Stem Cell Institute, University of Minnesota, Minneapolis, MN, USA. [3]Department of Molecular Genetics, Weizmann Institute of Science, Rehovot, Israel. [4]Paul and Sheila Wellstone Muscular Dystrophy Center, University of Minnesota, Minneapolis, MN, USA. [5]NorthStar Genomics, Eagan, MN, USA. [6]These authors contributed equally: Satyabrata Das, Naoko Koyano-Nakagawa. [7]These authors jointly supervised this work: Mary G. Garry, Daniel J. Garry. *e-mail: garry002@umn.edu; garry@umn.edu

CRISPR–Cas9 gene editing[12] (Supplementary Fig. 4). Embryos ($n = 898$) were cloned using somatic cell nuclear transfer (SCNT) and transferred to seven synchronized gilts[13]. At embryonic day 18 (E18), embryos ($n = 24$) were collected and analyzed using morphological and immunohistochemical analyses, FACS, hematopoietic colony-forming assays and quantitative PCR with reverse transcription (RT–qPCR) techniques (Fig. 1). Morphologically, *ETV2*$^{-/-}$ embryos were growth retarded and appeared pale as compared to stage-matched wild-type controls (Fig. 1a,b). Immunohistochemical analysis using the TIE2 and VWF antisera, which stain endothelial lineages, revealed the presence of vasculature in the wild-type embryos (Fig. 1c,e), which was completely absent in the null embryo (Fig. 1d,f). In the wild-type embryo, we observed TIE2$^+$ vessels in the yolk sac containing blood cells, while these cells were completely absent in the null embryos (Fig. 1g,h). By contrast, GATA4, DESMIN, NKX2-5 and smooth muscle actin (SMA), which stain the cardiac lineage, were present in the hearts of both the wild-type and *ETV2*-null embryos (Fig. 1c–f). Using FACS (Supplementary Fig. 5), the wild-type embryos displayed a CD45$^+$CD31$^+$ hematopoietic population and a CD31$^+$CD45$^-$ endothelial population, but both cell populations were absent in the null embryos (Fig. 1i,j). After co-culture with OP9 cells, the CD45$^+$ hematopoietic population and the CD31$^+$ endothelial population expanded from wild-type embryos, but not from *ETV2*-null embryos (Fig. 1k,l). Furthermore, methylcellulose assays revealed an absence of hematopoietic colony-forming units in *ETV2*-null embryos (Fig. 1m). Additionally, we confirmed the lack of hematoendothelial lineages in the *ETV2*-null embryos using RT–qPCR (Fig. 1n–q). *NKX2-5* and *HAND2* transcripts were increased in the *ETV2*-null embryos (Fig. 1r,s), similar to the observation in mouse null embryos[4]. Collectively, these studies demonstrate that porcine *ETV2*-null embryos lack hematoendothelial lineages and phenocopy the *Etv2*-null mouse[3–7].

Having defined the null phenotype, we assessed whether porcine endothelial and hematopoietic lineages of the *ETV2* knockout could be complemented in a cell-autonomous fashion. First, we used green fluorescent protein (GFP)-labeled porcine blastomeres as donor cells and examined their viability and integration into porcine host parthenogenetic embryos (parthenogenotes are developmentally incompetent embryos that are generated by the activation of a mature oocyte) and long-term culture in vitro (Supplementary Fig. 6). In these experiments, two GFP-labeled blastomeres were injected into day 4 pig morulae and examined every 48 h (Supplementary Fig. 6a–d). Although the number of embryos containing GFP$^+$ cells decreased over time (Supplementary Fig. 6c), the number of GFP$^+$ cells within embryos increased two- to five-fold (Supplementary Fig. 6b,d). These results indicate that the injected GFP blastomeres survive and proliferate in the developing blastocysts. Immunohistochemical staining revealed that the donor cells contributed to both OCT4$^+$CDX2$^-$ and OCT4$^+$CDX2$^+$ populations, which represent the inner cell mass and trophectoderm, respectively (Supplementary Fig. 6e), and confirmed that donor blastomeres express markers for both lineages in the host environment.

Having confirmed the integration of GFP blastomeres into parthenogenetic embryos, we performed complementation of *ETV2*-null embryos. *ETV2*-null embryos and GFP-labeled wild-type embryos were separately generated by SCNT. On day 4 of culture, *ETV2*-null embryos were injected with GFP-labeled wild-type blastomeres and transferred into synchronized gilts. The phenotype of the complemented E18 embryos ranged from those that were indistinguishable from *ETV2*-null embryos to those morphologically similar to wild-type embryos (Supplementary Fig. 7a). Examination of a well-developed embryo revealed that GFP$^+$ cells were distributed throughout the body and completely lined or decorated all of the vascular structures (Supplementary Fig. 7b–f). In the hematopoietic lineage, GFP signal was visible in all blood cells examined (Supplementary Fig. 7g,h). We quantitatively analyzed the contribution of GFP$^+$ cells to other lineages using immunohistochemistry. All TIE2$^+$ endothelial cells co-localized with GFP, whereas only a small subpopulation of SM22$^+$ smooth muscle cells, neuroepithelial cells, mesenchymal cells and intestinal cells were co-localized with GFP (Supplementary Fig. 7d–m). Complemented embryos harvested at E24 and full-term stages were subsequently examined and we were able to confirm that endothelial and hematopoietic lineages were complemented exclusively by the donor GFP$^+$ cells and that the lethality of the *ETV2* null had been rescued (Fig. 2 and Supplementary Fig. 8).

Next, we evaluated the development of pig parthenogenotes with and without injection of hiPSCs in three porcine media. We observed that parthenogenetic embryos developed equally well in PZM-MU2 and NCSU-23, but less efficiently in PZM-5 (Supplementary Fig. 9a; Methods). We noted that a substantial portion of injected hiPSCs underwent apoptosis in the porcine culture conditions. Thus, we tested whether we could support survival and proliferation of hiPSCs by an admixture of hiPSC medium with porcine medium. NCSU-23 and PZM-MU2 media were mixed with mTeSR 1 medium at various ratios and the survival and proliferation of three hiPSC lines were quantified after 72 h at 37 °C and 38.5 °C (Supplementary Fig. 9b–g). We observed improved survival and proliferation of all hiPSC lines at both 37 °C and 38.5 °C when the medium contained at least 20% mTeSR 1. Therefore, we determined that 80% PZM-MU2 and 20% mTeSR 1 at 38.5 °C (corresponding to the in vivo porcine temperature) was optimal for hiPSC survival and proliferation. Using these conditions, we observed that the number of parthenogenotes retaining live hiPSCs, as well as the number of hiPSCs within the parthenogenotes, decreased within the first 2 d after injection (Supplementary Fig. 9h,i). We examined whether the timing of hiPSC injection affects parthenogenote development and found no differences across conditions (Supplementary Fig. 9j,k).

Next, we developed methods to unambiguously identify human cells in the porcine host (Supplementary Fig. 10). Parthenogenotes were injected with DiI- or 5-ethynyl-2′-deoxyuridine (EdU)-labeled hiPSCs and cultured until they reached the blastocyst stage, fixed and examined by fluorescence microscopy for EdU or human nuclear antigen (HNA) expression. A comparison of DiI and anti-HNA immunohistochemistry confirmed that the HNA antibody specifically detected the injected hiPSCs (Supplementary Fig. 10a–c). Likewise, 100% of the EdU-prelabeled hiPSCs were detected with the HNA antibody (Supplementary Fig. 10d–g). We established two independent histological methods for the detection of human cells insofar as human and pig pancreatic sections were stained using genomic in situ hybridization with a primate-specific *ALU* probe or immunohistochemically using an anti-HNA antibody (Supplementary Fig. 10h–k). To quantify the human cell contribution, we used primer pairs specific to human *ALU* (Yb8) and mitochondrial cytochrome B genomic sequences. These primers detected human genomic DNA mixed with porcine DNA at 1:100,000 and 1:100 ratios, respectively (Supplementary Fig. 10l,m).

Using the optimized conditions, we injected four hiPSCs into porcine parthenogenotes and examined integration into blastocysts. After 48 h of culture, we found that hiPSCs had integrated with the host cells and connected via cell-adhesion molecules (E-cadherin or connexin-43; Fig. 3a–d). To examine whether a functional connection was established between hiPSCs and host cells, we injected hiPSCs preloaded with DiI and calcein. DiI does not spread between cells, whereas calcein diffuses through gap junctions. We found GFP$^+$ embryos in which calcein spread from hiPSCs into the host cells (Fig. 3e–h). This calcein transfer to porcine cells was not due to hiPSC death (resulting in dye release), because injection of lysate from calcein-loaded and mechanically disrupted hiPSCs did not result in labeling of host cells. Although the frequency of calcein transfer was low in chimeric embryos (found in less than

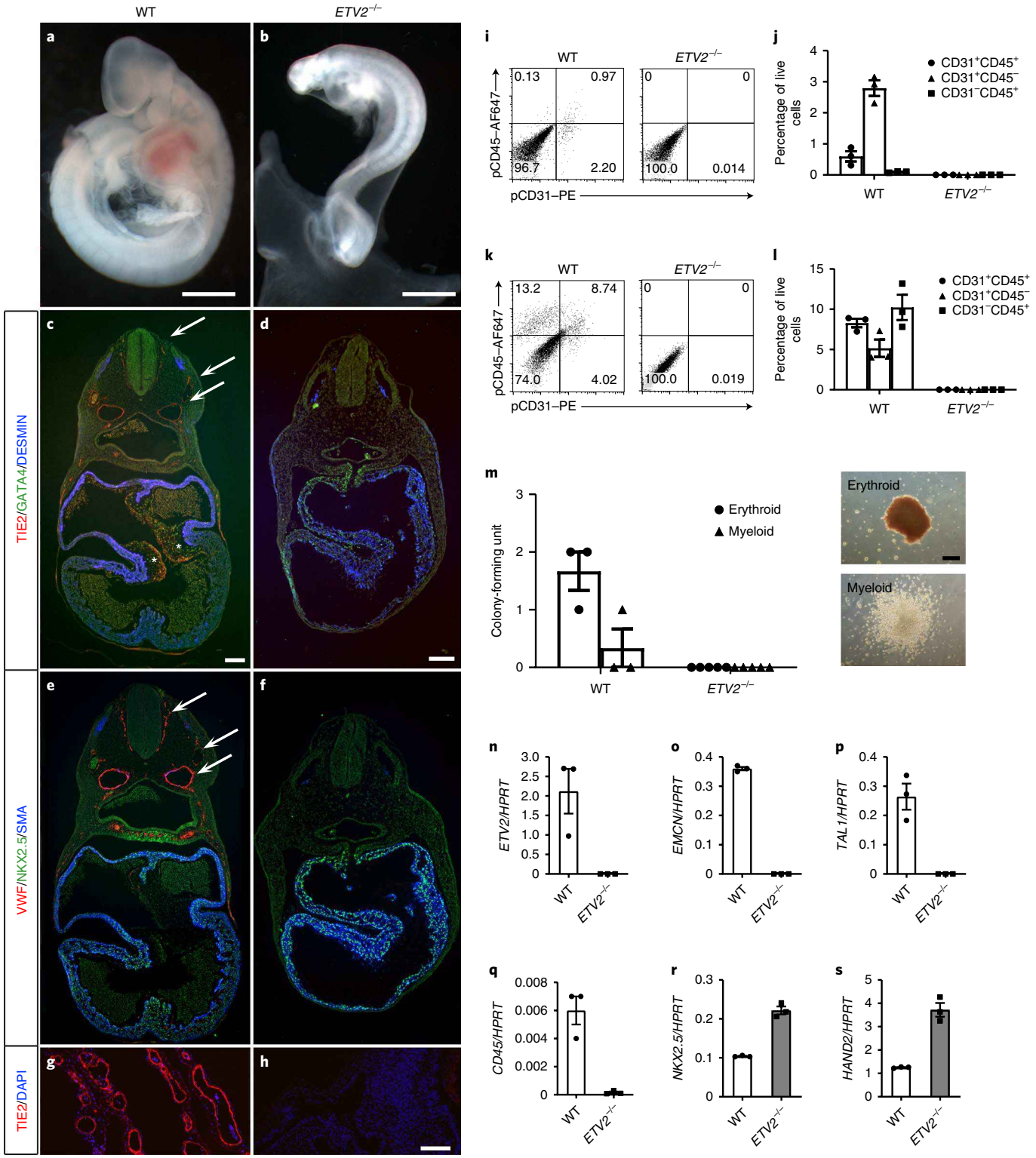

Fig. 1 | Porcine *ETV2*$^{-/-}$ embryos lack the hematopoietic and endothelial lineages and recapitulate the mouse phenotype. a–h, Whole-mount view (**a**,**b**) and cross sections (**c**–**h**) of wild-type (**a**,**c**,**e**,**g**) and *ETV2*$^{-/-}$ (**b**,**d**,**f**,**h**) embryos at E18. A total of 898 embryos were transferred to pseudopregnant gilts and 24 *ETV2*-null embryos were obtained from three independent *ETV2*-null porcine fibroblast clones and analyzed by whole-mount imaging. These E18 *ETV2*-null embryos were examined immunohistochemically (independently repeated, $n=7$). Sections were stained with antibodies against TIE2 (**c**,**d**,**g**,**h**) and VWF (**e**,**f**) to label the hematoendothelial lineages, and GATA4 and DESMIN (**c**,**d**) and NKX2-5 and SMA (**e**,**f**) to label the cardiac lineages. **g**,**h**, Yolk sac sections. Arrows point to endothelial cells. The asterisk denotes the cardiac cushion. Scale bars, 1 mm (**a**,**b**), 100 μm (**c**–**h**). **i**–**l**, FACS analysis of blood lineage from dissociated embryos ($n=3$ for the wild type and $n=5$ for *ETV2*$^{-/-}$). Representative plots (**i**,**k**) and quantification from wild-type and *ETV2*$^{-/-}$ embryos (**j**,**l**) are shown. **m**, Methylcellulose colony-forming assay reveals the complete absence of hematopoietic units in *ETV2*$^{-/-}$ embryos ($n=3$ for the wild type and $n=5$ for *ETV2*$^{-/-}$). **n**–**s**, Quantification of *ETV2* (**n**), *EMCN* (**o**), *TAL1* (**p**), *CD45* (**q**), *NKX2-5* (**r**) and *HAND2* (**s**) transcripts using RT-qPCR analysis (three wild-type and five *ETV2*-null embryos were used for the qPCR analysis and the data shown are in triplicate for each embryo). Error bars indicate mean ± s.e.m.

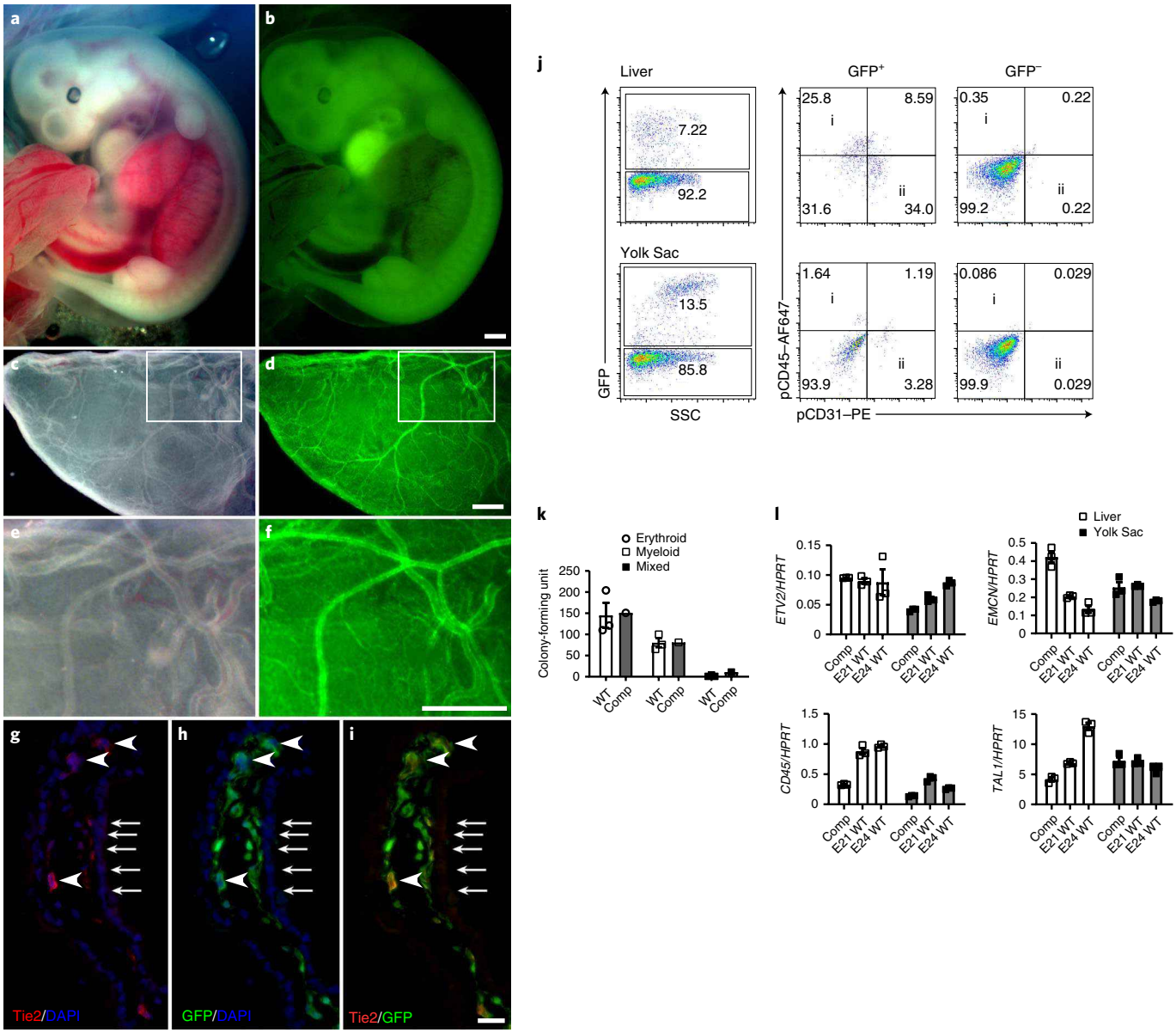

Fig. 2 | Complementation of *ETV2*$^{-/-}$ embryos (E24). A total of 1,322 wild-type–*ETV2*-null porcine complemented embryos were transferred to pseudopregnant gilts and eight wild-type–*ETV2*-null porcine complemented embryos were analyzed at distinct embryonic stages (Supplementary Fig. 7). **a**–**d**, Embryos were harvested and whole mounts were observed by brightfield (**a**) and epifluorescence (**b**) microscopy. Endothelial localization of EYFP was observed in yolk sac vessels (**c**–**f**). Boxed areas of **c** and **d** are enlarged in **e** and **f**, respectively. **g**–**i,** Immunohistochemical staining of a cross section of the yolk sac revealed that TIE2^{+} endothelial cells were GFP^{+} (arrowheads), whereas trophectoderm cells were GFP^{-} (arrows). **j**, FACS analysis of the dissociated embryo. Both hematopoietic (quadrant i) and endothelial (quadrant ii) populations in the fetal liver (top panels) and the yolk sac (top panels) were GFP^{+}. **k**, Methylcellulose assay of the complemented liver cells from one embryo showed comparable numbers of colony-forming units as compared to three biologically independent age-matched wild-type controls. **l**, RT-qPCR demonstrated that levels of *ETV2*, *EMCN*, *CD45* and *TAL1* were increased in liver and yolk sac of the complemented embryo. Data shown are in triplicate for each embryo (mean ± s.e.m.).

1% of the embryos), we unequivocally demonstrate that hiPSCs can directly integrate with the porcine host. Next, we examined whether hiPSCs could proliferate in the porcine host in the long term. To examine this possibility, we established parthenogenote culture conditions that sustained developmental progression up to 10 d. Two GFP-labeled hiPSCs were injected into a porcine parthenogenote. While the number of chimeric embryos decreased over time, those that contained viable cells had increased numbers of hiPSCs (Supplementary Fig. 11a–c), similar to the porcine GFP blastomeres delivered into porcine parthenogenotes (Supplementary Fig. 6c,d). Taken together, these results suggest that although there is an initial reduction of hiPSC viability (Supplementary Fig. 9h,i), if hiPSCs successfully integrate into the porcine environment, then they survive and proliferate.

We undertook embryonic complementation using hiPSCs to examine the integration of hiPSCs in vivo. Singularized hiPSCs were injected into *ETV2*-null blastocysts (hiPSC–*ETV2*-null porcine embryos), which were transferred to surrogate gilts. Embryos were analyzed between E17 and E18. Human cells were detected in embryos by quantitative PCR analysis of genomic DNA. We transferred 1,670 hiPSC–*ETV2*-null porcine embryos to 16 surrogate gilts and harvested 23 embryos or embryonic tissue. Using qPCR, we detected human DNA in 12 of these embryo or embryonic tissue samples (Fig. 3i; $P < 0.05$, top ten are presented). Of

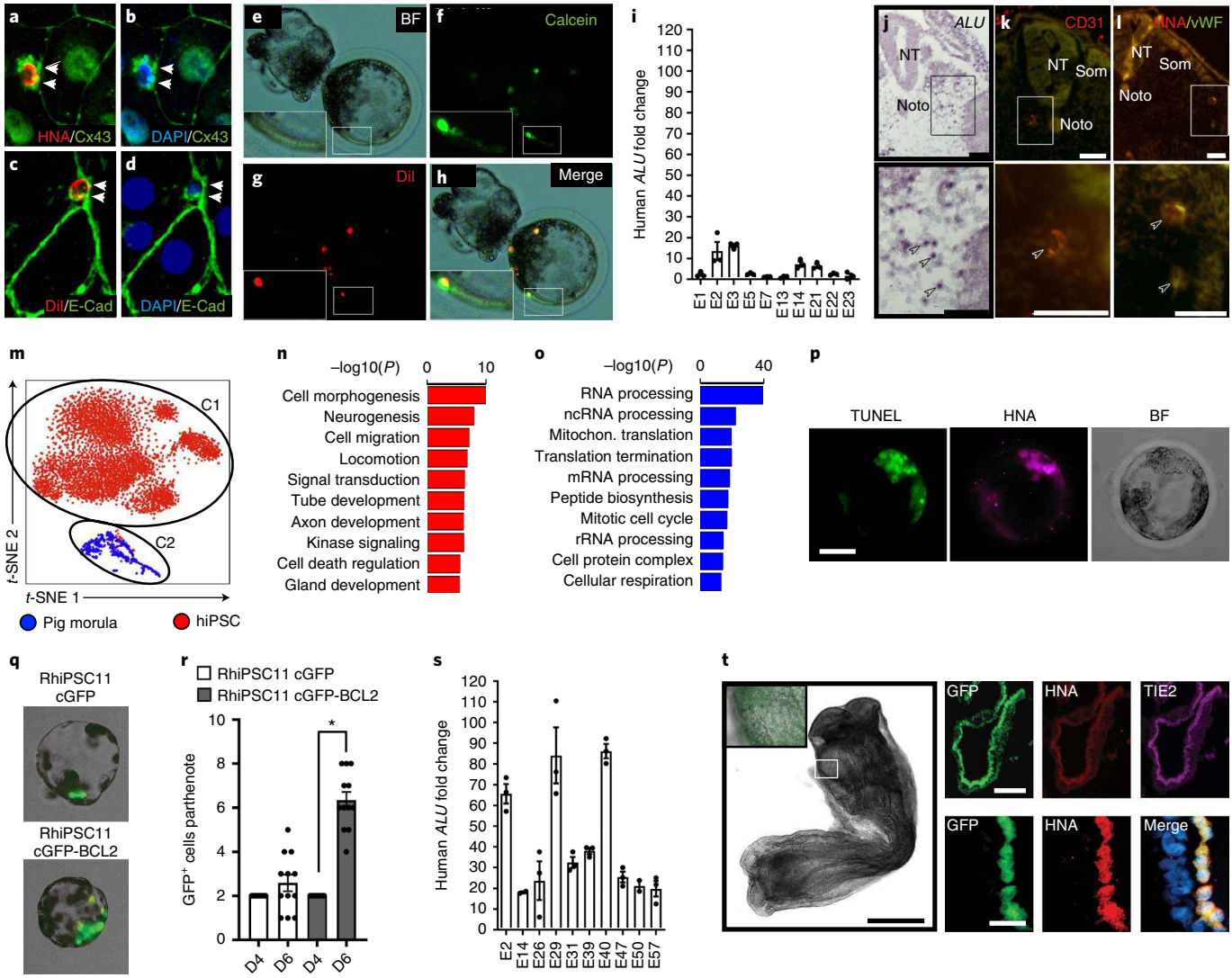

Fig. 3 | Complementation of ETV2$^{-/-}$ embryos with hiPSCs. a–d, Porcine parthenogenotes injected with DiI-labeled hiPSCs at the morula stage and cultured in vitro for 48 h. Embryos were fixed and stained with antibodies to connexin-43 (CX43) and E-cadherin (E-CAD), which detect both human and porcine antigens. Co-localization with HNA was also used to identify hiPSCs. Arrowheads point to attachment sites of hiPSC to host cells ($n=400$). **e–h**, Parthenogenotes were injected with hiPSCs loaded with calcein and DiI and examined live after 48 h for the spread of calcein. Inset shows calcein spreading from DiI-labeled hiPSCs to the neighboring host cells ($n=289$). **i–l**, Analysis of *ETV2*-mutant embryos injected with hiPSCs. *ETV2*$^{-/-}$ blastocysts ($n=1,670$) were injected with hiPSCs, transferred to 16 synchronized gilts and analyzed at E18. Total DNA from 23 embryos or embryonic tissue were analyzed for human DNA content. The top ten embryos containing detectable human DNA as compared to background pig DNA are shown. The human *ALU* fold change shown in **i** is defined as the ratio between the observed PCR signal and the baseline t_0. According to the one-sample location test (Z test), any observed *ALU* PCR signal above this threshold or baseline would represent a significantly higher *ALU* PCR signal as compared to the mean (μ), with $P<0.05$ (Methods). Data represent mean ± s.e.m. Sections were analyzed by *ALU* in situ hybridization (**j**), immunohistochemistry against human CD31 (**k**), HNA and human VWF (**l**). **j**,**k**,**l**, Bottom panels show increased magnification of the boxed areas in the top panels, respectively. ALU$^+$ cells were found scattered within the embryo (arrowheads in **j** bottom), and cells that express human antigens were identified (arrowheads in **k**,**l** bottom). Noto, notochord; NT, neural tube; Som, somite. Scale bars, 50 µm. **m–o**, scRNA-seq of porcine morulae ($n=592$ cells) and hiPSCs ($n=5,000$ cells) using the Seurat algorithm to account for the batch effect with the definition of two clusters (**m**), which were characterized using the Gene Ontology (GO) classification (**n**,**o**). **p**, Following the delivery of hiPSCs into porcine parthenogenotes and 48 h of culture (BF) a subpopulation of the hiPSCs (HNA$^+$ cells) were noted to undergo apoptosis (TUNEL$^+$ cells). **q–t**, BCL2 overexpression increases the efficiency of human–porcine chimeras. **q**, Representative blastocyst images (day 6) showing a marked increase in the number of cGFP-BCL2 hiPSCs (bottom) versus control GFP hiPSCs (top) in porcine parthenogenote blastocysts. **r**, Quantification of GFP$^+$ hiPSCs per parthenogenote following the delivery of control cGFP hiPSCs versus cGFP-BCL2 hiPSCs. Note the marked increase in the number of GFP$^+$ cells per parthenogenote with delivery of the cGFP-BLC2 hiPSCs. These experiments were performed three times independently with similar results. Porcine parthenogenotes with GFP$^+$ hiPSCs were counted ($n=12$). The asterisk denotes statistical significance determined by one-way analysis of variance and non-parametric test ($P=6\times10^{-6}$). Data represent mean ± s.e.m. **s**,**t**, Analysis of *ETV2*-mutant embryos injected with cGFP-BLC2 hiPSCs. *ETV2*$^{-/-}$ blastocysts ($n=1,321$) were injected with cGFP-BLC2 hiPSCs, transferred to 11 synchronized gilts and analyzed at E17. **s**, Total DNA from 63 embryos or embryonic tissue were analyzed for human DNA content. The top ten embryos containing detectable human DNA as compared to background pig DNA are shown. The statistical test used is same as **i**. **t**, Brightfield whole-mount image of the cGFP-BCL2:ETV2-null complemented E18 embryo with an inset demonstrating GFP fluorescence (left). Cryosections were analyzed using immunohistochemistry for GFP, HNA and TIE2 demonstrating co-expression (right top). Immunohistochemistry for GFP, HNA and DAPI (blue) demonstrate co-expression in the nuclear compartment of the E17 chimera (right bottom). These experiments were repeated independently in triplicate with similar results.

these 12 embryos, five were growth retarded and were used entirely for genomic PCR analysis. Of the remaining seven, we observed that four hiPSC–*ETV2*-null porcine embryos collected had cell nuclei positive for the *ALU* sequence (by in situ hybridization or HNA immunohistochemistry; Fig. 3j,l). Of note, in adjacent sections, we observed cells positive for HNA, human-specific CD31 and VWF (Fig. 3k,l). These parallel lines of evidence indicate that hiPSC-derived cells were responsive to the developmental cues and differentiated to the endothelial lineage. To identify the distinct molecular programs in porcine morulae and hiPSCs, we used single-cell RNA sequencing (scRNA-seq) to profile 592 porcine morulae cells and compared these results with published hiPSC scRNA-seq datasets ($n = 5{,}000$ cells). We used Seurat alignment to remove the species differences between human and porcine data. Two clusters were identified (C1, hiPSCs only; and C2, pig morulae and hiPSCs) and pathway analysis revealed that the cells from cluster C1 had increased cell death regulation (Fig. 3m–o). We found that decreased efficiency of human–porcine chimeras using parthenogenotes was due to programmed cell death of the injected hiPSCs (Fig. 3p).

To increase the efficiency of chimera formation we used gene-editing technologies to overexpress the antiapoptotic factor BCL2 in copGFP (cGFP)-expressing hiPSCs (Supplementary Fig. 12). We examined whether cGFP-BCL2 hiPSCs had increased efficiency for human–porcine chimeras in vitro. Two cGFP-labeled BCL2 hiPSCs were injected into a porcine morula parthenogenote, cultured and noted to have increased cGFP$^+$ parthenogenotes and increased number of cGFP$^+$ cells per parthenogenote (Fig. 3q,r). We then examined the capacity of cGFP-labeled BCL2 hiPSCs for embryonic complementation using the *ETV2*-null porcine morula, which were transferred to synchronized gilts. We analyzed embryos at E17 and detected human cells in embryos by qPCR analysis of genomic DNA. We transferred 1,321 hiPSC–*ETV2*-null porcine embryos to 11 synchronized gilts and harvested 63 embryos or embryonic tissue. Using qPCR, we detected human DNA in 51 of these embryos or embryonic tissue, (Fig. 3s; $P < 0.05$, top ten are presented). Our data show that BCL2 overexpression in hiPSCs results in more than a fivefold increase in the efficiency of human–porcine chimeras as compared to wild-type hiPSCs (Fig. 3i,s and Supplementary Fig. 13e) correlating to approximately 1:2,000 cells (Supplementary Fig. 13).

Using whole-mount brightfield and epifluorescence microscopy, we observed cGFP expression in the chimeric porcine embryos (Fig. 3t). Using immunohistochemistry we observed co-expression of cGFP, HNA and TIE2 (Fig. 3t) and noted that cGFP-expressing cells co-expressed HNA in the nuclear compartment at high magnification (Fig. 3t). These parallel lines of evidence indicate that BCL2 overexpression in hiPSCs results in increased efficiency of human–porcine chimeras (Supplementary Fig. 13a,b) and that these BCL2-overexpressing hiPSCs differentiate to the endothelial lineage. Quantification of the immunohistochemical images showed that 91% of the cGFP-expressing cells were TIE2$^+$, whereas essentially all of the TIE2$^+$ cells co-expressed cGFP (Supplementary Fig. 13c,d). While the efficiency of human–pig chimera complementation technologies remains limited, BCL2-overexpressing hiPSCs increased the capacity to produce interspecies chimeras (Supplementary Fig. 13e).

Our data demonstrate the successful use of complementation strategies and the feasibility of engineering human–porcine chimeric embryos. Future studies will be needed to further increase the efficiency of chimerism, to ensure lack of contribution of hiPSC derivatives to other organs and to address other potential immunogenicity issues of the humanized organ. We also note that the safety of overexpressing an antiapoptotic factor in hiPSCs for generation of organs for xenotransplantation has not been assessed.

In summary, we demonstrate that *ETV2*-null pig embryos lack hematopoietic and vascular lineages and that these embryos can be rescued in a cell-autonomous fashion in both mice and pigs. Given reports of successful exogenous organ production such as pancreas and kidney[1,2,14,15], our data support the notion that the *ETV2* mutation could be combined with other gene mutations to generate exogenous organs with reduced immunogenicity.

Online content

Any methods, additional references, Nature Research reporting summaries, source data, extended data, supplementary information, acknowledgements, peer review information; details of author contributions and competing interests; and statements of data and code availability are available at https://doi.org/10.1038/s41587-019-0373-y.

Received: 22 March 2018; Accepted: 26 November 2019;
Published online: 24 February 2020

References

1. Kobayashi, T. et al. Generation of rat pancreas in mouse by interspecific blastocyst injection of pluripotent stem cells. *Cell* **142**, 787–799 (2010).
2. Usui, J. I. et al. Generation of kidney from pluripotent stem cells via blastocyst complementation. *Am. J. Pathol.* **180**, 2417–2426 (2012).
3. Ferdous, A. et al. Nkx2-5 transactivates the Ets-related protein 71 gene and specifies an endothelial/endocardial fate in the developing embryo. *Proc. Natl Acad. Sci. USA* **106**, 814–819 (2009).
4. Rasmussen, T. L. et al. ER71 directs mesodermal fate decisions during embryogenesis. *Development* **138**, 4801–4812 (2011).
5. Koyano-Nakagawa, N. et al. Etv2 is expressed in the yolk sac hematopoietic and endothelial progenitors and regulates *Lmo2* gene expression. *Stem Cells* **30**, 1611–1623 (2012).
6. Rasmussen, T. L. et al. VEGF/Flk1 signaling cascade transactivates *Etv2* gene expression. *PLoS One* **7**, e50103 (2012).
7. Rasmussen, T. L. et al. Etv2 rescues *Flk1* mutant embryoid bodies. *Genesis* **51**, 471–480 (2013).
8. Wu, J. et al. Interspecies chimerism with mammalian pluripotent stem cells. *Cell* **168**, 473–486 (2017).
9. Lee, D. et al. ER71 acts downstream of BMP, Notch, and Wnt signaling in blood and vessel progenitor specification. *Cell Stem Cell* **2**, 497–507 (2008).
10. Hadjantonakis, A. K., Macmaster, S. & Nagy, A. Embryonic stem cells and mice expressing different GFP variants for multiple non-invasive reporter usage within a single animal. *BMC Biotechnology* **2**, 11 (2002).
11. Shi, X. et al. The transcription factor Mesp1 interacts with cAMP-responsive element binding protein 1 (Creb1) and coactivates Ets variant 2 (*Etv2*) gene expression. *J. Biol. Chem.* **290**, 9614–9625 (2015).
12. Whitworth, K. M. et al. Use of the CRISPR/Cas9 system to produce genetically engineered pigs from in vitro-derived oocytes and embryos. *Biol. Reprod.* **91**, 78 (2014).
13. Giraldo, A. M., Ball, S. & Bondioli, K. R. Production of transgenic and knockout pigs by somatic cell nuclear transfer. *Methods Mol. Biol.* **885**, 105–123 (2012).
14. Wu, J. et al. Generation of human organs in pigs via interspecies blastocyst complementation. *Reprod. Domest. Anim.* **51**, 18–24 (2016).
15. Yamaguchi, T. et al. Interspecies organogenesis generates autologous functional islets. *Nature* **542**, 191–196 (2017).

Methods

Animal assurance. The scientific merit, the ethical justification of the experimental studies and the animal welfare as outlined in the studies were reviewed and approved by the Institutional Review Board, Institutional Animal Care and Use Committee and Stem Cell Research Oversight panels at the University of Minnesota and Midwest Research Swine.

Mice. *Etv2*-EYFP[4], *Etv2*$^{-/-}$ (ref. [3]) and *Etv2*-conditional-knockout mice (CKO)[11] have been described elsewhere. In brief, the *Etv2*-EYFP mouse line was generated using the 3.9-kb *Etv2* promoter cloned into the pEYFP-1 promoterless vector and transgenic mouse lines were generated using standard techniques in the FVB background. The *Etv2*$^{-/-}$ line was generated using the ES cell line (141.1H7; 129X1/SvJ×129S1/Sv)F1-Kitl<+>), which contains the insertion of the gene-trapping construct (pGep-SD5; International Gene Trap Consortium) at the exon–intron boundary of exon five of *Etv2* and were maintained by crossing with C57BL6 mice. The *Etv2* CKO mice were generated with homologous recombination of a vector that harbored a 1.8-kb target region, which included exons five through seven flanked by LoxP sites and a neomycin cassette flanked by flippase-recognition target cassettes. The targeting vector was linearized and electroporated into C57BL/5×129/SvEv hybrid ES cells to generate chimerae. A line was established via germline inheritance and neomycin was removed via matings to *Flp1*. The *Etv2* CKO mice were maintained by breeding with C57Bl6 mice. *Etv2*^{DKI} was generated by deleting the conditional allele with a germline Cre-driver, *EIIA*-Cre[11]. *Etv2*$^{DKI/+}$ (hemi) and *Etv2*$^{DKI/KO}$ (null) embryos were generated by crossing *Etv2*^{DKI} with the *Etv2*$^{-/-}$.

Embryonic stem cells–embryoid body system. The *Etv2*-null ES cell line and a control line derived from littermates have been reported previously[7]. Mesodermal differentiation and FACS analysis were carried out as described[16].

Human induced pluripotent stem cells. Sources of hiPSCs are: shiPSC9-1 (foreskin fibroblast; gift from J. Dutton (University of Minnesota)), hBF-ACHE (fibroblasts), human skin embryonic fibroblasts (8FW; GM00011 from Coriell Institute) and SC12-034 (mesenchymal stem cell; G. Daley (Harvard Medical School)). These hiPSC lines tested negative for mycoplasma contamination. hiPSCS were cultured in mTeSR 1 or TeSR-E8 on Matrigel-coated plastic plates as previously described[17], and passaged at least 2 d before usage, in a density to reach 70–80% confluency at the time of harvest. Cells were rinsed with PBS without calcium and magnesium, dissociated by TrypLE treatment for 5 min at 37 °C (Thermo Fisher Scientific), suspended in a prewarmed DMEM–F12 medium containing 15% serum and collected in a conical tube. Cells were collected by centrifugation for 5 min at 200*g* and resuspended in mTeSR 1 containing ROCK inhibitor (10 μM Y27632). For in vitro tracing experiments, hiPSCs were pulsed with mTeSR 1 containing 10 μM EdU for 24 h or 5 μM DiI (Molecular Probes) for 2 h, washed in PBS and dissociated before injection.

Genomic targeting of human induced pluripotent stem cells. RhiPSC11 cell line was dissociated to a single-cell suspension using TrypLE Express (Gibco), centrifuged, resuspended and transfected using the Human Stem Cell Nucleofector kit 2 (Lonza) according to the manufacturer's instructions. *CLYBL* locus targeting using transcription activator-like effector nuclease was done as previously described[18]; pZT-C13-L1, pZT-C13-R1 and pC13N-iCAG.copGFP plasmids were purchased from Addgene (plasmids 62196, 62197 and 66578, respectively). Colonies were then selected using neomycin at 50 μg ml^{-1}. The BCL2-puro donor plasmid was edited in house and knocked-in to the AAVS1 locus using the CRISPR–Cas9 method with a guide RNA (gRNA; GTCACCAATCCTGTCCCTAG). Colonies were selected with 0.5 μg ml^{-1} puromycin.

Guide RNA design and cloning. Candidate gRNA sequences for pig *ETV2* were designed using an online tool (http://crispr.mit.edu/). gRNAs flanking the 5′ (CAGCAGACGTCACAATCCGC) and 3′ (TGGTACCGACTAGATCCTCC) regions of the *ETV2* gene were designed and cloned into the mammalian-codon-optimized Cas9-expressing plasmid pX459 (Addgene, 48139) as described elsewhere[19].

Fetal fibroblast collection, tissue culture and nucleofection. Porcine fetal tissue was collected on day 35 of gestation to create cell lines as described previously[12]. In brief, each fetus was minced and digested in 20 ml of digestion medium (DMEM containing L-glutamine and 1 g l^{-1} D-glucose (Cellgro) supplemented with 200 U ml^{-1} collagenase (Sigma) and 25 Kunitz units per milliliter DNaseI (Sigma)) for 4 h at 38.5 °C. After digestion, fetal fibroblast cells were washed and cultured with DMEM containing 15% FBS and 40 μg ml^{-1} gentamicin. After overnight culture, the cells were trypsinized and frozen at −80 °C in aliquots in FBS with 10% dimethyl sulfoxide overnight and moved to liquid nitrogen for long-term storage. Pig fibroblasts were maintained at 38.5 °C at 5% CO_2 in DMEM supplemented with 15% FBS, 5 ng ml^{-1} basic fibroblast growth factor and 10 mg ml^{-1} gentamicin. These cells were kept at a low passage (passage less than ten) and characterized on the basis of their morphology. The Nucleofector 2b device (Lonza) was used to deliver the all-in-one CRISPR–Cas9 plasmid using program U-012. Approximately 600,000 cells were nucleofected with 6 μg of plasmid using the Basic Nucleofector kit for primary mammalian fibroblasts (#VPI-1002). Nucleofected cells were cultured for 2 or 3 d at 38.5 °C and then analyzed for gene-editing efficiency and plated for colonies.

Dilution cloning. Two or three days after nucleofection, 50 cells were seeded onto 10-cm dishes and cultured for 2 weeks. Colonies were picked on day 14 after transfection by applying 10-mm autoclaved cloning cylinders around each colony. Colonies were rinsed with PBS and collected via trypsin treatment; then resuspended in DMEM. Two-thirds of the resuspended colony were transferred into a well of a 24-well plate and the remaining third was collected into a PCR tube. The cell pellets were resuspended in 10 μl of lysis buffer (40 mM Tris, pH 8.9, 0.9% Triton X-100 and 0.4 mg ml^{-1} proteinase K (NEB)), incubated at 65 °C for 30 min for cell lysis, followed by 85 °C for 10 min to inactivate the proteinase K. Expanded clones were collected and cryopreserved.

Analysis of *ETV2* gene edits. Primers flanking the intended sites (listed in Supplementary Table 1) were used to conduct PCR using GoTaq Green Master Mix (Promega) with 1 μl of the cell lysate. Clones having deletion of the entire *ETV2* gene were identified from the PCR amplicons by agarose gel electrophoresis. Four different PCR assays were used to identify biallelic *ETV2*-null clones. All of the PCR conditions included an initial denaturation of 98 °C for 2 min followed by 33 cycles of 10 s at 98 °C, 30 s at 58 °C and 30 s at 72 °C. A small PCR product of ~580 base pairs using primers flanking the two gRNAs would confirm biallelic deletion of the gene as the full 3,160-base-pair product cannot be generated with the short extension time used in the amplification cycle. Further PCR reactions, using primers flanking each gRNA, were performed to confirm the absence of an amplicon. Another PCR reaction, using a primer pair internal to the two gRNAs, was performed to rule out *ETV2* translocation in the genome. PCR products from clones showing biallelic deletions were cloned into pCR2.1 TOPO (Life Technologies) vector and sequenced using Sanger sequencing to confirm the deletion of *ETV2*.

Medium components. Medium components used for short-term porcine parthenogenote culture are listed in Supplementary Table 2. mTeSR 1 (STEM CELL Technologies) was used for hiPSC culture and media-mixing experiments.

Parthenogenetic embryos. Activated oocytes were obtained from a commercial supplier (DeSoto Biosciences) or generated in house by using oocytes aspirated from gilt ovaries obtained from local farms. In brief, for the DeSoto parthenogenesis, cumulus oocyte complexes were collected from mature sows and placed in maturation medium. Oocytes were denuded in a hyaluronidase solution (2 mg ml^{-1}) 40–44 h after maturation. Mature oocytes were electrically activated with two DC pulses of 1.5 kV cm^{-1} for 30 μs each, delivered by a BTX Electro Cell Manipulator (Biotechnologies and Experimental Research). For in-house parthenogenesis, cumulus oocytes from gilts were matured for 40–42 h and denuded in a hyaluronidase solution (0.3 mg ml^{-1}). They were activated by two DC pulses of 1.2 kV cm^{-1} for 30 μs. After activation, the presumptive pseudozygotes were incubated for 4 h in PZM-MU2 medium containing 7.5 μg ml^{-1} cytochalasin B. DeSoto embryos were loaded in vials containing pre-equilibrated NCSU-23 medium and shipped overnight in a portable incubator at 38.5 °C. Parthenogenotes were cultured in a 500-μl drop of PZM-MU2 medium at 38.5 °C under 5% CO_2 and 5% O_2 (covered with mineral oil to avoid evaporation).

Generation of *ETV2*-mutant embryos. *ETV2*-mutant or GFP embryos were generated by SCNT as previously described[20,21]. In brief, pig primary oocytes complexes aspirated from ovarian follicles were cultured in vitro for 40 to 42 h in medium-199 (Corning, 10-060-CV) with 10 ng ml^{-1} epidermal growth factor (Sigma, E4127), 0.5 μg ml^{-1} follicle stimulating hormone (Sigma, F2293), 0.5 μg ml^{-1} luteinizing hormone (Sigma, L5269), 3.05 mM D-glucose (Sigma, G6152), 0.91 mM Na-pyruvate (Sigma, P4562), 0.57 mM L-cysteine (Sigma, C7352), 40 ng ml^{-1} basic fibroblast growth factor (Sigma, F0291), 20 ng ml^{-1} insulin-like growth factor (Prospec, CYT-022), 20 ng ml^{-1} leukemia inhibitory factor (Millipore, LIF1050), 10 μg ml^{-1} gentamicin (Gibco, 15710-064) and 0.1% polyvinyl alcohol (Sigma, P8136) for 40–42 h at 38.5 °C and 5% CO_2 in humidified air[12]. The matured oocytes with extrusion of the first polar body were enucleated in a manipulation medium drop by aspirating the polar body with approximately 10% of cytoplasm adjacent to the polar body together using micromanipulators. The manipulation medium consisted of medium-199 (Gibco, 31100-027) supplemented with 30 mM NaCl (Sigma, S5886), 595 μM $NaHCO_3$ (Sigma, S5761), 2.9 mM HEPES (Sigma, H3784) and 10 μg ml^{-1} gentamicin (Gibco, 15710-064). *ETV2*-mutant or GFP transgenic fibroblasts prepared in advance on a tissue culture plate were harvested on the day of SCNT. The single fibroblast was placed into the perivitelline space of each enucleated oocyte and the nucleus of the fibroblast was fused with each oocyte by two direct current pulses of 1.2 kV cm^{-1} for 30 μs in 300 mM mannitol (Sigma, M9546) supplemented with 0.5 mM HEPES, 0.1 mM $CaCl_2$ (Sigma, C7902) and $MgCl_2$ (Sigma, M0250). The fused embryos were activated in 0.2 mM thimerosal (Sigma, T8784) for 10 min and in 8 mM dithiothreitol (Sigma, D5545) for 30 min[22].

For the in vitro culture of pig SCNT embryos PZM-MU2 medium was used and in the initial 14–16 h of culture, a histone deacetylase inihibitor (Scriptaid, 0.5 µM; Sigma, S7817) was supplemented to enhance the epigenetic reprogramming of the embryos[23,24].

Injections of blastomeres and hiPSCs into parthenogenotes. Preparation of blastomeres and injection are described below. For long-term culture (Supplementary Fig. 6), two GFP-labeled blastomeres were injected into embryos at the day 4 compacted morula stage and cultured in PZM-MU2 at 38.5 °C under 5% CO_2 and 5% O_2 (covered with mineral oil to avoid evaporation). For hiPSC injection studies, two to five hiPSCs (as specified in the text) were injected and cultured in a medium cocktail containing PZM-MU2:mTeSR 1 (80:20), 10% heat inactivated FBS, 5 mM glucose and 10 mM glycine at 38.5 °C under 5% CO_2 and 5% O_2 (covered with mineral oil)[25].

***ETV2*-mutant embryo complementation (injection of blastomeres and hiPSCs into *ETV2*-mutant embryos and in vivo transfer).** The injection for embryo complementation was done 4 d after SCNT. GFP embryo blastomeres were inserted into the *ETV2*-mutant embryos for embryo complementation (a small subpopulation of embryos were provided by RCI/MOFA). The GFP blastomeres were prepared after decompaction in PZM-HEPES with 0.1 mM EDTA (Invitrogen, 15575-038) and the zona pellucida was removed by pipetting in 0.2% pronase (Roche, 10165921001) in PBS until it was completely removed. The dissociated blastomeres were washed once in PZM-HEPES supplemented with 20% FBS and twice in PZM-HEPES medium. The *ETV2*-mutant embryos were decompacted in the same way. The GFP blastomeres were inserted using a microcapillary, which has an inner diameter of 40 µm, through the perforation on the zona pellucida of the *ETV2*-mutant embryos made using the laser system (Hamilton Thorne). For in vitro long-term culture (Supplementary Fig. 6), two to eight blastomeres (half the number of host blastomeres) were injected into 4- to 16-cell-stage embryos in PZM-HEPES medium, respectively. Injections of cGFP$^+$-hiPSCs or cGFP$^+$-BCL2 hiPSCs were performed using the same procedure and injecting four hiPSCs per embryo. Transfer of embryos into hormonally primed gilts was performed using published methods[21].

Immunohistochemical analysis of sections and embryos. Immunohistochemistry was performed on sections as previously described[5]. For analysis of embryos, parthenogenotes cultured in vitro were fixed in 4% paraformaldehyde on ice for 10 min, washed three times in 0.05% Tween-20 in PBS (PBST) and permeabilized in 0.1% Triton X-100 in PBS for 10 min. Afterward embryos were washed three times in PBST and transferred to blocking solution (10% normal donkey serum in PBST) for 1 h. After blocking, embryos were incubated at 4 °C overnight with the primary antibody diluted in blocking solution. On the second day, the embryos were washed three times with PBST and incubated in the secondary antibody conjugated with fluorophores for 1 h. After incubation, the embryos were washed with PBST three times and counterstained with 10 µg ml^{-1} Hoechst 33342 or DAPI for 10 min.

Antibodies. The following antibodies were used: GFP (1:500; Abcam, ab13970), endomucin (1:400; Abcam, ab106100), TIE2 (1:200; eBioscience, 14-5987), GATA4 (1:500; R&D Systems, AF2606), DESMIN (1:400; Abcam, ab6322), SMA (1:100; Abcam, ab7817), SM22 (1:500; Abcam, ab14106), NKX2-5 (1:800; Santa Cruz, sc-8697), connexin-43 (1:200; Abcam, ab11370), E-cadherin (1:200; BD Biosciences, 610181), OCT4 (1:400, clone H-134; Santa Cruz, sc9081), CDX2 (1:200; Biogenex, MU392-A-UC), GFP (1:400; Abcam, ab13970), HNA (1:100; Abcam, ab191181), BrdU (1:500; AbD Serotec, OBT0030), human CD31 (1:400; BD Biosciences, 550274), VWF (1:200; Novocastra, 404705) and BCL2 (1:500, clone C21; Santa Cruz, sc-783; immunoblot). Stained sections were dehydrated and mounted in DPX (Electron Microscopy Sciences 13510).

FACS analysis. Dissociation and immunostaining of the cells from embryoid bodies were performed as previously described and analysis was performed using a FACSAria sorter (BD Biosciences)[4]. Pig and mouse embryos were washed with PBS without Ca^{2+} and Mg^{2+}, then dissociated with collagenase type II (1 mg ml^{-1}) and dispase (2 mg ml^{-1}) (Thermo Fisher Scientific) for 10 min, followed by addition of trypsin and EDTA (0.05%) for 5 min at 37 °C. The antibodies used for FACS included: anti-mouse Flk1–APC (1:300, clone Avas12a1; eBioscience, 17-5821-81), anti-mouse Tie2–PE (1:1,000, clone TEK4; eBioscience, 12-5987-83), anti-mouse CD41–PECy7 (1:500, clone MWReg30; eBioscience, 25-0411-82), anti-pig CD31–PE (1:500, clone LCI-4; Biorad, MCA1746PE) and anti-pig CD45–Alexa Fluor 647 (1:500, clone K252.1E4; Biorad, MCA1222A647). Propidium iodide (1:1,000; Thermo Fisher Scientific, P3566) was used to exclude dead cells. All data acquired were analyzed with FlowJo v.10.4.2 (FlowJo).

Hematopoietic assay. Following dissociation as described above, cells were washed once with PBS, filtered through a 40-µm strainer and plated for hematopoietic colony-forming culture or co-cultured with mouse OP9 bone marrow stromal cells. For fetal liver samples, cells were mechanically homogenized and lysed with RBC lysis buffer (BD Biosciences). For methylcellulose colony-forming assay, 60,000 cells were transferred onto human methylcellulose base medium (HSC002, R&D systems) with 20 ng ml^{-1} each of sSCF, swine interleukin (IL)-3, swine granulocyte macrophage colony-stimulating factor, swine erythropoietin, swine IL-6 and human thrombopoietin. All swine cytokines were purchased from KingFisher Biotech and human thrombopoietin was purchased from Shenandoah Biotechnology. Hematopoietic colonies were counted after 12–14 d. For OP9 co-culture assay, 3×10^5 cells were cultured on a monolayer of mouse OP9 stromal cells in α-MEM with 20% FBS, swine stem cell factor (50 ng ml^{-1}), human thrombopoietin (50 ng ml^{-1}), swine IL-3 (20 ng ml^{-1}), swine granulocyte macrophage colony-stimulating factor (20 ng ml^{-1}) and swine IL-6 (20 ng ml^{-1}). Medium was replaced every 3 d. At day 7, whole co-cultured cells were trypsinized, filtered with a 40-µm cell strainer and analyzed by flow cytometry.

Genomic in situ hybridization. In situ hybridization was done according to the standard protocols with NBT-BCIP as a substrate[26]. The human *ALUII* probe was purchased from Biogenex.

EdU detection of parthenogenotes. The Click-iT EdU Alexa Fluor 647 Imaging kit (Thermo Fisher Scientific) was used to visualize EdU-labeled hiPSCs.

Quantitative PCR with reverse transcription. Genomic DNA was purified using a Wizard genomic DNA purification kit (Promega). RNA was purified using RNeasy mini kit (Qiagen). Supplementary Table 1 includes all primers used for qPCR. The GFP primer was obtained from ABI (Mr04329676_mr).

Human *ALU* fold change calculations. We used human-specific *ALU* PCR primers. Importantly, the *ALU* elements are not present in the pig genome. Initially, we determined a baseline number t_0 representing the absence of *ALU* sequence. We performed *ALU* PCR from the pig (non-chimeric) genome and added two standard deviations (σ) of the PCR signal to the mean (μ), that is, $t_0 = \mu + 2\sigma$. The human *ALU* fold change shown in Fig. 3i,s and Supplementary Fig. 13e was defined as the ratio between the observed PCR signal and the baseline t_0. According to the one-sample location test (Z test), any observed *ALU* PCR signal above this threshold or baseline would represent a significantly higher *ALU* PCR signal as compared to the mean (μ), with $P < 0.05$.

Imaging and statistical analysis. Sections were imaged using a laser confocal microscope (Zeiss LM510). Whole-mount parthenogenotes were placed in PBS covered with mineral oil in a glass-bottom dish and imaged on a fluorescence microscope (Olympus IX83), an inverted confocal microscope (Nikon, A1R confocal laser microscope system) or a deconvolution microscope (Nikon TiE). For quantification, at least ten fields of different levels of sections were randomly chosen and counted. Statistical analyses were done with one-way analysis of variance.

TetraZ assay. hiPSC were cultured in mTeSR and passaged onto 48-well multiwell clusters coated with Matrigel to achieve 15–20% confluency. When the cells reached 50% confluency, medium was replaced with 300 µl of mixed medium (NCSU-23 or PZM-MU2 and mTeSR 1 at the indicated ratios) and cultured at the indicated temperatures. Medium was replaced daily. At 48 h after plating, cells were fed with fresh mTeSR 1 for 1 h, then 20 µl of TetraZ reagent (Biolegend, TetraZ Cell Counting kit) was added to each well and further incubated for 4 h at 37 °C. At the end of incubation, supernatants were assayed following the manufacturer's instructions. Assays were performed in quadruplicate.

Calcein transfer from injected hiPSCs to pig blastomeres through gap junctions. Before dissociation, shiPS9.1 cells were incubated with 2 µM Calcein AM (Invitrogen, L3224) and 5 µM DiI (Molecular Probes, V-22885) diluted in mTeSR 1 containing 10 µM ROCK inhibitor for 20 min. Day 4 parthenogenotes were decompacted in 0.1 mM EDTA diluted with PZM-HEPES. Four cells loaded with Calcein AM and labeled with DiI were injected into each parthenogenote. The injected parthenogenotes were cultured in mTeSR 1 containing 10 µM ROCK inhibitor for 4 h, at which time the culture medium was replaced with a mixture of media containing 80% PZM-MU2 and 20% mTeSR 1 and the parthenogenotes were cultured for an additional 24 h at 38.5 °C. After 24 h, live parthenogenotes were examined using fluorescence microscopy (Olympus IX83).

Data analysis. No data were excluded from these studies and all attempts at replication for standard assays (that is, FACS, qPCR, methylcellulose colony-forming assays and immunohistochemistry) were successful. Investigators were blinded whenever possible (during, for example, FACS analysis, manual cell counting, culture studies and qPCR). However embryos were processed in the order that they were delivered in to maximize preservation and to inform subsequent steps, which limited investigator blinding in some instances.

Single-cell RNA sequencing of porcine morulae. Two- to four-cell pig embryos were harvested from naturally bred pigs 2–3 d after mating. The uterus was harvested at the abattoir and was subsequently flushed with warm PBS to remove embryos. Harvested two- to four-cell embryos were cultured in PGEM-MU2

medium for 1–2 d at 38.5 °C in an incubator with 5% CO_2 and 5% O_2 until they developed to compacted morula stage. At this stage the morulae were treated with pronase to remove zona pellucida, followed by EDTA treatment for decompaction. Each single cell was picked manually into individual wells of a 96-well PCR plate on ice. First-strand cDNA synthesis and full-length double-stranded cDNA amplification was performed using the SMART-Seq v4 Ultra Low Input RNA kit for sequencing according to the recommended protocol. Each cell was collected in a volume of ~1 µl. A quarter of the recommended amount of each reagent was used for the cDNA synthesis and double-stranded cDNA amplification reactions were tuned for optimal results with low input RNA from a single cell. Amplified double-stranded cDNAs were purified and validated by the bioanalyzer. Library preparation was performed using the Illumina kit according to manufacturer's protocols. All libraries were sequenced using 75-bp paired-end sequencing on NextSeq apparatus (Illumina). The sequencing reads were mapped to the porcine genome (susScr3) using TopHat (v.2.0.13) and the raw read counts were obtained by HTSeq (v.0.6.0) with default parameters. Cells with less than 500,000 paired reads or less than 50% of mapping rate were removed, resulting in 592 high-quality single cells for analysis. The scRNA-seq data of 18,787 human iPSCs were obtained from Nguyen et al.[27]. The raw reads were mapped to human genome (hg19) using TopHat (v.2.0.13)[28] and the raw read counts were obtained by HTSeq (v.0.6.0)[29] with default parameters. To combine the hiPSC data with porcine data, we mapped the porcine genes to human orthologs using the R's BiomaRt package, and only kept the porcine genes that could be uniquely mapped to human orthologs. We randomly sampled 5,000 hiPSC single cells and combined them with the 592 porcine morula single cells. Seurat alignment[30] was utilized to remove the batch effects of human and porcine cells.

Reporting Summary. Further information on research design is available in the Nature Research Reporting Summary linked to this article.

Data availability

The scRNA-seq data that support the findings of this study have been deposited in NCBI Sequence Read Archive (SRA) database under accession number PRJNA577880. All data will be made available by the authors upon reasonable request. All unique materials used in these studies are readily available from the authors or from commercial sources (Supplementary Tables 1 and 2). Gene-edited primary cell lines are limited in number but will be made available pending their supply.

References

16. Iacovino, M. et al. A conserved role for Hox paralog group 4 in regulation of hematopoietic progenitors. *Stem Cells Dev.* **18**, 783–792 (2009).
17. Chen, G. et al. Chemically defined conditions for human iPSC derivation and culture. *Nat. Methods* **8**, 424–429 (2011).
18. Cerbini, T. et al. Transcription activator-like effector nuclease (TALEN)-mediated CLYBL targeting enables enhanced transgene expression and one-step generation of dual reporter human induced pluripotent stem cell (iPSC) and neural stem cell (NSC) lines. *PloS one* **10**, e0116032 (2015).
19. Koyano-Nakagawa, N. et al. Feedback mechanisms regulate *Ets Variant 2 (Etv2)* gene expression and hematoendothelial lineages. *J. Biol. Chem.* **290**, 28107–28119 (2015).
20. Lai, L. & Prather, R. S. Production of cloned pigs by using somatic cells as donors. *Cloning Stem Cells* **5**, 233–241 (2003).
21. Sembon, S. et al. A simple method for producing tetraploid porcine parthenogenetic embryos. *Theriogenology* **76**, 598–606 (2011).
22. Machaty, Z., Wang, W. H., Day, B. N. & Prather, R. S. Complete activation of porcine oocytes induced by the sulfhydryl reagent, thimerosal. *Biol. Reprod.* **57**, 1123–1127 (1997).
23. Whitworth, K. M., Zhao, J., Spate, L. D., Li, R. & Prather, R. S. Scriptaid corrects gene expression of a few aberrantly reprogrammed transcripts in nuclear transfer pig blastocyst stage embryos. *Cell. Reprogram.* **13**, 191–204 (2011).
24. Zhao, J. et al. Significant improvement in cloning efficiency of an inbred miniature pig by histone deacetylase inhibitor treatment after somatic cell nuclear transfer. *Biol. Reprod.* **81**, 525–530 (2009).
25. Redel, B. K. et al. Glycine supplementation in vitro enhances porcine preimplantation embryo cell number and decreases apoptosis but does not lead to live births. *Mol. Reprod. Dev.* **83**, 246–258 (2016).
26. Allard, J. et al. Immunohistochemical toolkit for tracking and quantifying xenotransplanted human stem cells. *Regen. Med.* **9**, 437–452 (2014).
27. Nguyen, Q. H. et al. Single-cell RNA-seq of human induced pluripotent stem cells reveals cellular heterogeneity and cell state transitions between subpopulations. *Genome Res.* **28**, 1053–1066 (2018).
28. Trapnell, C. et al. Differential gene and transcript expression analysis of RNA-seq experiments with TopHat and Cufflinks. *Nat. Protoc.* **7**, 562–578 (2012).
29. Anders, S., Pyl, P. T. & Huber, W. HTSeq-a Python framework to work with high-throughput sequencing data. *Bioinformatics* **31**, 166–169 (2015).
30. Butler, A., Hoffman, P., Smibert, P., Papalexi, E. & Satija, R. Integrating single-cell transcriptomic data across different conditions, technologies, and species. *Nat. Biotechnol.* **36**, 411–420 (2018).

Acknowledgements

This work was supported by a grant from the Department of Defense (grant no. 11763537 to D.J.G.) and Minnesota Regenerative Medicine (to D.J.G.). We thank J. Dutton (University of Minnesota) and G. Daley (Harvard Medical School) for providing hiPSC lines. We thank C. Chapman for assisting with the hiPSC culture studies, E. Skie for genetic analyses, Y. Ren and C. Walter for the FACS analysis, and B. Coffin, A. Arnason, L. Meisner and D. Ly for morphological analyses. We thank A. Caplan for critical comments during the course of these studies. We acknowledge the Mouse Genetics Laboratory, Veterinary Diagnostic Laboratory and the University Imaging Center at the University of Minnesota, NorthStar Genomics, Recombinetics, DeSoto Biosciences, grafikalabs (http://grafikalabs.com/) and MOFA Global for their technical assistance. We also thank R. Prather and the National Swine Resource and Research Center at the University of Missouri for providing technical training and assistance (U42 OD011140).

Author contributions

N.K.-N., M.G.G. and D.J.G. conceived the project and S.D., N.K.-N., D.Y., M.G.G. and D.J.G. wrote the manuscript. S.D., N.K.-N., T.R., O.G., S.K., B.N.S., G.M., X.P., K.-D.C., P.P., W.G., J.H.H., D.M. and C.V.W. designed and performed experiments, and analyzed the data. N.K.-N., M.G.G. and D.J.G. supervised the project. All authors commented on and edited the final version of the paper.

Competing interests

D.J.G. and M.G.G. are co-founders of NorthStar Genomics.

Additional information

Supplementary information is available for this paper at https://doi.org/10.1038/s41587-019-0373-y.

Correspondence and requests for materials should be addressed to M.G.G. or D.J.G.

nature research

Corresponding author(s): Garry, D.J.

Last updated by author(s): Nov 7, 2019

Reporting Summary

Nature Research wishes to improve the reproducibility of the work that we publish. This form provides structure for consistency and transparency in reporting. For further information on Nature Research policies, see Authors & Referees and the Editorial Policy Checklist.

Statistics

For all statistical analyses, confirm that the following items are present in the figure legend, table legend, main text, or Methods section.

n/a	Confirmed
☐	☒ The exact sample size (*n*) for each experimental group/condition, given as a discrete number and unit of measurement
☐	☒ A statement on whether measurements were taken from distinct samples or whether the same sample was measured repeatedly
☐	☒ The statistical test(s) used AND whether they are one- or two-sided *Only common tests should be described solely by name; describe more complex techniques in the Methods section.*
☐	☒ A description of all covariates tested
☐	☒ A description of any assumptions or corrections, such as tests of normality and adjustment for multiple comparisons
☐	☒ A full description of the statistical parameters including central tendency (e.g. means) or other basic estimates (e.g. regression coefficient) AND variation (e.g. standard deviation) or associated estimates of uncertainty (e.g. confidence intervals)
☐	☒ For null hypothesis testing, the test statistic (e.g. *F*, *t*, *r*) with confidence intervals, effect sizes, degrees of freedom and *P* value noted *Give P values as exact values whenever suitable.*
☒	☐ For Bayesian analysis, information on the choice of priors and Markov chain Monte Carlo settings
☒	☐ For hierarchical and complex designs, identification of the appropriate level for tests and full reporting of outcomes
☒	☐ Estimates of effect sizes (e.g. Cohen's *d*, Pearson's *r*), indicating how they were calculated

Our web collection on statistics for biologists contains articles on many of the points above.

Software and code

Policy information about availability of computer code

Data collection	The single cell RNA-seq data of 18,787 human iPSCs were obtained from Nguyen et al. The raw reads were mapped to human genome (hg19) using TopHat (v2.0.13) and the raw read counts were obtained by HTSeq (v0.6.0) with default parameters.
Data analysis	The sequencing reads of porcine morula single cells were mapped to porcine genome (susScr3) using TopHat (v2.0.13) and the raw read counts were obtained by HTSeq (v0.6.0) with default parameters. The cells with less than 500,000 paired reads or less than 50% of mapping rate were removed, resulting in 592 high quality single cells for analysis. To combine the hiPSC data with porcine data, we mapped the porcine genes to human orthologs using R's BiomaRt package, and only kept the porcine genes that can be uniquely mapped to the human orthologs. We randomly sampled 5,000 hiPSC single cells and combined them with 592 porcine morula single cells. The Seurat (v3.0) alignment was utilized to remove the batch effects of human and porcine cells. Other software used for data analysis are FlowJo ver. 10.4.2, GraphPad Prism.

For manuscripts utilizing custom algorithms or software that are central to the research but not yet described in published literature, software must be made available to editors/reviewers. We strongly encourage code deposition in a community repository (e.g. GitHub). See the Nature Research guidelines for submitting code & software for further information.

Data

Policy information about availability of data

All manuscripts must include a data availability statement. This statement should provide the following information, where applicable:

- Accession codes, unique identifiers, or web links for publicly available datasets
- A list of figures that have associated raw data
- A description of any restrictions on data availability

The single cell RNA-seq data that support the findings of this study have been deposited in NCBI Sequence Read Archive (SRA) database with the project accession number PRJNA577880. All data will be available upon request. All unique materials used in these studies are readily available from the authors or from commercial

sources (see Tables 1 and 2). Gene edited primary cell lines are limited in number but will be available pending their supply.

Field-specific reporting

Please select the one below that is the best fit for your research. If you are not sure, read the appropriate sections before making your selection.

☒ Life sciences ☐ Behavioural & social sciences ☐ Ecological, evolutionary & environmental sciences

For a reference copy of the document with all sections, see nature.com/documents/nr-reporting-summary-flat.pdf

Life sciences study design

All studies must disclose on these points even when the disclosure is negative.

Sample size	No sample size calculation was performed rather studies were routinely performed at least in triplicate for these SCNT and large animal studies.
Data exclusions	No data excluded
Replication	All attempts at replication for standard assays (i.e. FACS, qPCR, methylcellulose colony assays, immunohistochemistry) were successful. These techniques were routinely performed at least in triplicate. We observed that the production of null embryos was reliable and reproducible. SCNT, chimerism and complementation data reflect low efficiencies that are well established in the field.
Randomization	Random allocation as possible.
Blinding	Investigators were blinded whenever possible (eg., FACS analysis, manual cell counting, culture studies, qPCR, etc.). Embryos were processed, however in the order that they were delivered to maximize preservation and it inform next steps which limited investigator blindness in some instances.

Reporting for specific materials, systems and methods

We require information from authors about some types of materials, experimental systems and methods used in many studies. Here, indicate whether each material, system or method listed is relevant to your study. If you are not sure if a list item applies to your research, read the appropriate section before selecting a response.

Materials & experimental systems

n/a	Involved in the study
☐	☒ Antibodies
☐	☒ Eukaryotic cell lines
☒	☐ Palaeontology
☐	☒ Animals and other organisms
☒	☐ Human research participants
☒	☐ Clinical data

Methods

n/a	Involved in the study
☒	☐ ChIP-seq
☐	☒ Flow cytometry
☒	☐ MRI-based neuroimaging

Antibodies

Antibodies used	The antibodies used for FACS included: anti-mouse Flkl-APC (1:300, clone Avas12al; eBioscience, 17-5821-81, Lot # E07311-1632), anti-mouse Tie2-PE (1:1000, clone TEK4; eBioscience, 12-5987-83, Lot # E01993-1635), anti-mouse CD41-PECy7 (1:500, clone MWReg30; eBioscience 25-0411-82, Lot # E07563-1632), anti-pig CD31-PE (1:500, clone LCl-4; Biorad MCA1746PE, Lot # INN1603) and anti-pig CD45 Alexa Fluor 647 (1:500, clone K252.1E4; Biorad MCA1222A647, Lot # 1602). The antibodies used for immunohistochemical purposes included: Green fluorescent protein (1:500, Abcam ab13970, Lot # GR236651-19), Endomucin (1:400, Abcam ab106100, Lot # GR278315-2), TIE2 (1:200, eBioscience 14-5987, Lot # E03128-1632), GATA4 (1:500, R&D systems AF2606, Lot # VAZC515101), DESMIN (1:400, Abcam ab6322, Lot # GR276481-3), SMA (1:100, Abcam ab7817, Lot#/Clone# 1A4), SM22 (1:500, Abcam ab14106, Lot # GR157642-1), NKX2-5 (1:800, Santa Cruz sc-8697, Lot # L2215), CONNEXIN 43 (1:200, Abcam ab11370, Lot # GR170975-25), E-CADHERIN (1:200, BD 610181, Lot#/Clone# 36/E-Cadherin), OCT4 (1:400, Santa Cruz sc9081, Lot # H-134), CDX2 (1:200, Biogenex MU392-A-5UC, Lot # MU392A0616), GFP (1:400, Abcam ab13970), HUMAN NUCLEAR ANTIGEN (HNA) (1:100, Abcam ab191181, Lot # GR227669-2), BrdU (1:500, AbD Serotec OBT0030, Lot#/Clone# BU1/75(ICR1)), human CD31 (1:400, BD Biosciences 550274, Lot # 5572), VWF (1:200, Novocastra Ncl-vwfp, Lot # 404705), TurboGFP (1:5,000, ThermoFisher PA5-22688), and BCL2 (1:500, C21 Santa Cruz sc-783; immunoblot).
Validation	This information is provided in the manuscript and includes data from the manufacturer's website and substitution controls.

Eukaryotic cell lines

Policy information about cell lines

Cell line source(s)	shiPSC9-1 (foreskin fibroblast, J. Dutton, Univ. of Minnesota), hBF-ACHE (fibroblasts, J. Hanna), human skin embryonic fibroblasts (8FW; GM00011 from Coriell Institute), SC12-034 (mesenchymal stem cell, G. Daley, Harvard Medical School). RhiPSC11 (Reprogrammed in our lab).
Authentication	Authentication procedures for cell lines produced are provided. These include cellular analysis using FACS and immunohistochemistry for pluripotency factors. Additional molecular analysis using qPCR for the pluripotency markers was used for cell line authentication. Karyotypic analysis was also performed.
Mycoplasma contamination	As outlined in the manuscript, all cell lines tested negative for mycoplasma contamination.
Commonly misidentified lines (See ICLAC register)	No commonly misidentified cell lines were used.

Animals and other organisms

Policy information about studies involving animals; ARRIVE guidelines recommended for reporting animal research

Laboratory animals	C57/B6 Female and male mice (2-8 months of age) were bred and the progeny were analyzed. Mixed strains of Landrace x Yorkshire x Duroc porcine gilts were used for the pig studies.
Wild animals	No wild animals were used in the study.
Field-collected samples	Study did not involve samples collected from the field.
Ethics oversight	IACUC (Institutional Animal Care and Use Committee) SCRO (Stem Cell Research Oversight)

Note that full information on the approval of the study protocol must also be provided in the manuscript.

Flow Cytometry

Plots

Confirm that:

☒ The axis labels state the marker and fluorochrome used (e.g. CD4-FITC).

☒ The axis scales are clearly visible. Include numbers along axes only for bottom left plot of group (a 'group' is an analysis of identical markers).

☐ All plots are contour plots with outliers or pseudocolor plots.

☐ A numerical value for number of cells or percentage (with statistics) is provided.

Methodology

Sample preparation	This information is provided in the manuscript.
Instrument	This information is provided in the manuscript.
Software	FlowJo Ver 10.4.2 (FloJo, LLC)
Cell population abundance	This information is provided in the manuscript.
Gating strategy	This information is provided in the manuscript.

☒ Tick this box to confirm that a figure exemplifying the gating strategy is provided in the Supplementary Information.